

Half-scan cone-beam CT fluoroscopy with multiple x-ray sources

Ying Liu^{a)}

Info & Images, 1405 Aburdeen Court, Iowa City, Iowa 52246

Hong Liu

Bioengineering Center, University of Oklahoma, Norman, Oklahoma 73019

Ying Wang

Info & Images, 3812 Chamberlyne Way, Norman, Oklahoma 73072

Ge Wang

Micro-CT Lab, Department of Radiology and Department of Biomedical Engineering, University of Iowa, Iowa City, Iowa 52242

(Received 13 December 2000; accepted for publication 3 May 2001)

To develop volumetric micro-CT fluoroscopy for small animal imaging, we have proposed a cone-beam system with multiple x-ray sources. In this paper, we extend Parker's single-source half-scan weighting scheme to the case of an odd number of x-ray sources that are equiangularly distributed, and apply it for half-scan Feldkamp-type reconstruction in this unique geometry. In the numerical simulation with the Shepp–Logan phantom, representative images indicate that the proposed half-scan Feldkamp-type algorithm produces temporal resolution significantly superior to that with a single x-ray source cone-beam system. © 2001 American Association of Physicists in Medicine. [DOI: 10.1118/1.1381549]

Key words: computed tomography (CT), multiple x-ray sources, half-scan, fan-beam, cone-beam, image reconstruction, fluoroscopy

I. INTRODUCTION

Although small animal models have been found indispensable in medical research, their potential has not been fully explored yet because often the animals have to be sacrificed for analysis. This prevents researchers from observing the natural or perturbed physiological/pathological processes *in vivo*. Biomedical imaging is the only approach for providing multidimensional data of interest in a noninvasive and repeatable fashion. Most biomedical imaging devices are tuned for human studies and have suboptimal performance for small animal studies. Therefore, it is desirable to scale down imaging systems for significantly improved images of mouse-sized objects.

Micro-CT systems have been proved useful for studying bony structures, organs, and tissues.¹ Because of its unique imaging capabilities and relatively low cost, micro-CT is a powerful imaging modality for small animal studies. Over the past several years, tremendous progress has been made in x-ray detector hardware, real-time/volumetric CT algorithms, and computing techniques. Development of a volumetric micro-CT fluoroscopy system with multiple x-ray sources has become feasible. This type of scanner would modify the concept and design of the Dynamic Spatial Reconstructor (DSR) developed at the Mayo Clinic.² Such a device could be a vital tool in biomedical laboratories for small animal studies and other applications, e.g., contrast-enhanced functional imaging.

Previously, we have proposed a top-level design for a cone-beam system with multiple x-ray sources (NIH R43RR15325). In this paper, we generalize Parker's half-

scan weighting scheme³ to the case of an odd number of x-ray sources, derive a half-scan Feldkamp-type reconstruction formula for this imaging geometry, and evaluate the new formula with numerical simulation.

II. HALF-SCAN FAN-BEAM WEIGHTING

The time span of the x-ray source scanning for collection of projection data used for image reconstruction determines the temporal resolution of reconstructed images. Therefore, in order to optimize CT temporal resolution we should minimize the angular range of the source by utilizing only one complete set of projection data. Assuming a single x-ray source and fan-beam geometry (diverging rays from the source are detected by a linear detector array), Parker derived a half-scan weighting scheme that combines data in doubly sampled regions smoothly and avoids the discontinuities at the borders of these regions.³

As shown in Fig. 1, the equiangular fan-beam geometry is assumed, where β denotes the angular position of an x-ray source, α the angular position of a detector, and Δ the fan-beam angle. Fig. 2 summarizes Parker's classic design of the single-source half-scan weighting function. In Fig. 2, the upper and lower triangles are sampled twice, hence the data in the two regions must be combined to make a unit contribution in image reconstruction. Specifically, the weighting scheme Parker proposed is expressed as follows:³

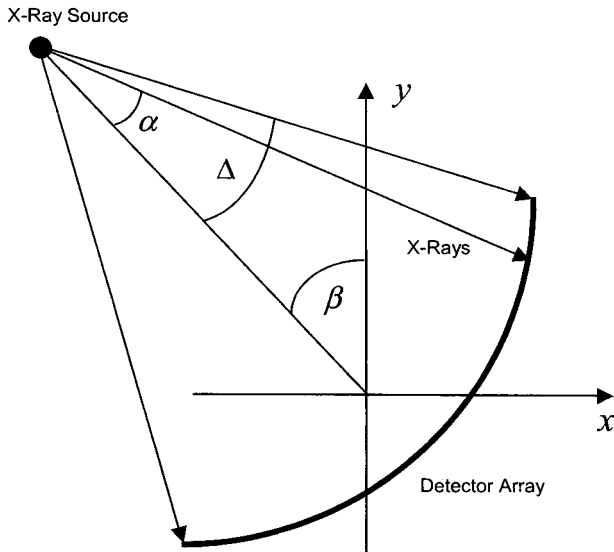


FIG. 1. Equiangular fan-beam geometry, in which diverging rays from the source are detected by a linear detector array with each detector extending the same angular increment.

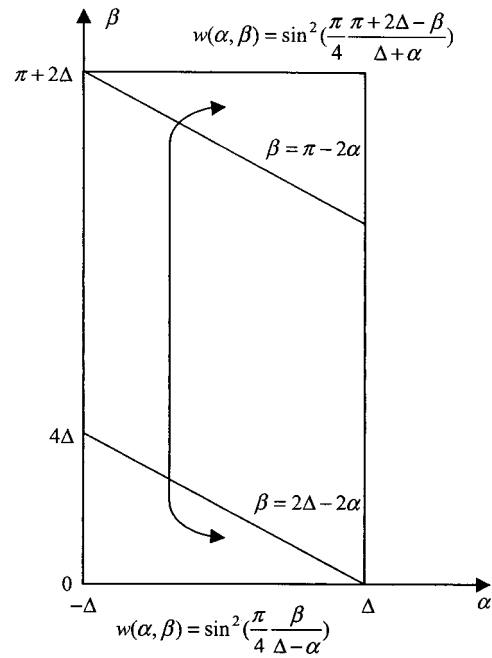


FIG. 2. Redundant regions in a fan-beam half-scan.

$$w(\alpha, \beta) = \begin{cases} \sin^2\left(\frac{\pi}{4} \frac{\beta}{\Delta - \alpha}\right), & 0 \leq \beta \leq 2\Delta - 2\alpha \\ \sin^2\left(\frac{\pi}{4} \frac{\pi + 2\Delta - \beta}{\Delta + \alpha}\right), & \pi - 2\alpha \leq \beta \leq \pi + 2\Delta \\ 1, & 2\Delta - 2\alpha \leq \beta \leq \pi - 2\alpha \end{cases} \quad (1)$$

In the case of an odd number N of x-ray sources that are symmetrically distributed with respect to the reconstruction system origin, for the optimal temporal resolution the minimum source scanning angular range should be used to collect a set of complete projection data. It can be proved that the minimum source angular range is $\pi/N + 2\Delta$, assuming that

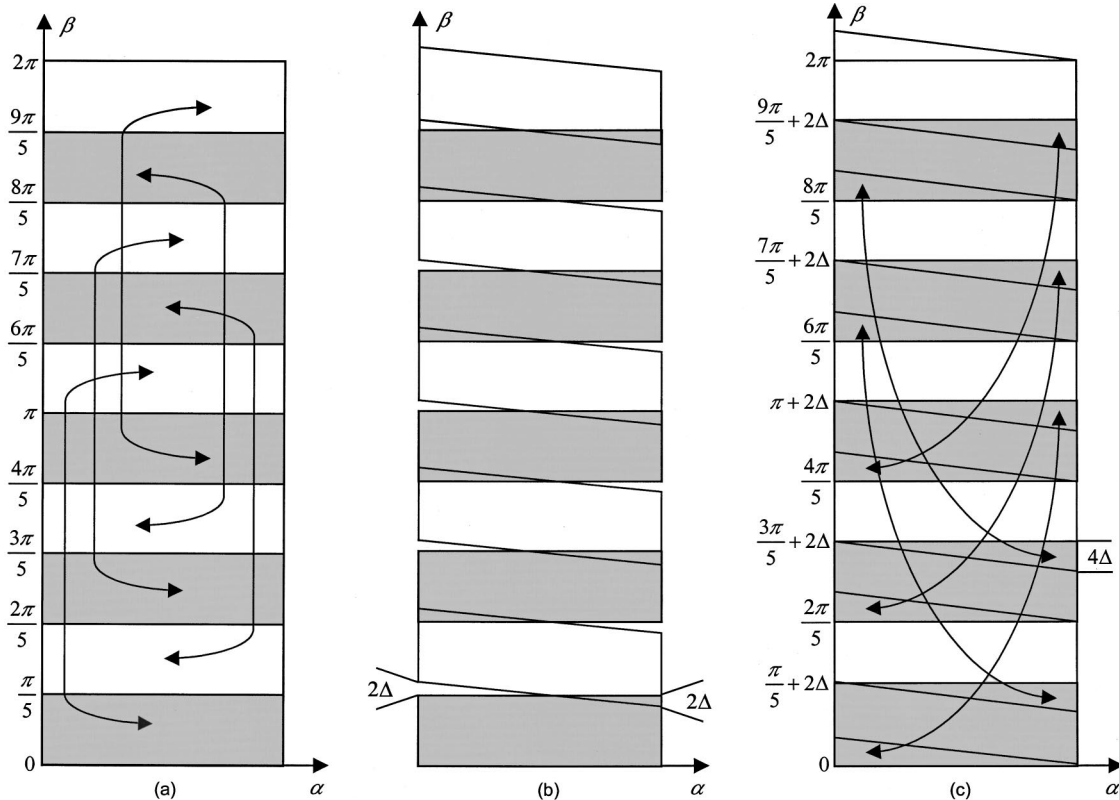


FIG. 3. Half-scan coverage with five x-ray sources. (a) Half-scan data coverage shown as the shaded regions in parallel-beam geometry, (b) insufficient data coverage in fan-beam geometry given the scanning range of (a), (c) sufficient data coverage in fan-beam geometry with the minimum scanning range $\pi/5 + 2\Delta$.

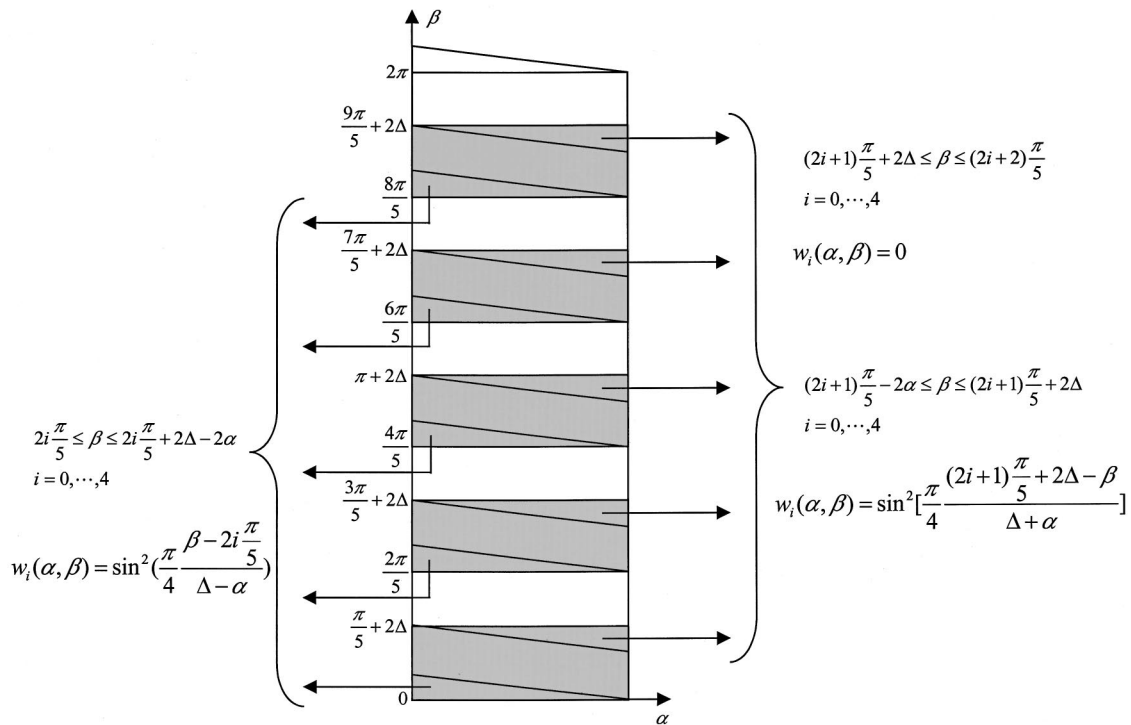


FIG. 4. Generalization of Parker's weighting scheme to the case of five x-ray sources.

$\Delta \leq \pi/2N$. This relationship is illustrated in Fig. 3. In Fig. 3(a), the minimum source angular range equals π/N in parallel-beam geometry. However, as shown in Fig. 3(b), with the same source angular range π/N there would be oversampled and undersampled triangular regions of height

2Δ . These defects are rectified in Fig. 3(c) in which the undersampled triangular regions are covered by increasing the source angular range from π/N to $\pi/N + 2\Delta$. Generalizing Parker's weighting scheme³ in the fashion illustrated in Fig. 4, we have the N weighting functions as follows:

$$w_i(\alpha, \beta) = \begin{cases} \sin^2\left(\frac{\pi}{4} \frac{\beta - 2i\frac{\pi}{N}}{\Delta - \alpha}\right), & 2i\frac{\pi}{N} \leq \beta \leq 2i\frac{\pi}{N} + 2\Delta - 2\alpha \\ \sin^2\left(\frac{\pi}{4} \frac{(2i+1)\frac{\pi}{N} + 2\Delta - \beta}{\Delta + \alpha}\right), & (2i+1)\frac{\pi}{N} - 2\alpha \leq \beta \leq (2i+1)\frac{\pi}{N} + 2\Delta \\ 0, & (2i+1)\frac{\pi}{N} + 2\Delta \leq \beta \leq (2i+2)\frac{\pi}{N} \\ 1, & \text{otherwise} \end{cases} \quad (2)$$

where $i=0, \dots, N-1$, N is an odd number. It can be verified that after the N -source half-scan weighting the weight is a unit at each location of the doubly sampled regions, and continuous at the boundaries of these redundant regions. Figure 5 presents weighting functions computed according to Eq. (2).

III. HALF-SCAN CONE-BEAM RECONSTRUCTION

Filtered backprojection is the standard image reconstruction method for x-ray CT. By Feldkamp-type reconstruction,

we refer to a one-dimensional filtration and three-dimensional backprojection mechanism for image reconstruction in cone-beam geometry.⁴⁻⁶ Although projection data are insufficient for accurate and reliable reconstruction of transverse sections using Feldkamp-type algorithms, it can be intuitively appreciated that data acquired along opposite geometric rays are partially redundant, since these rays would be identical in the absence of any fan-beam tilting angle and any longitudinal translation between the x-ray tube and the object being scanned.

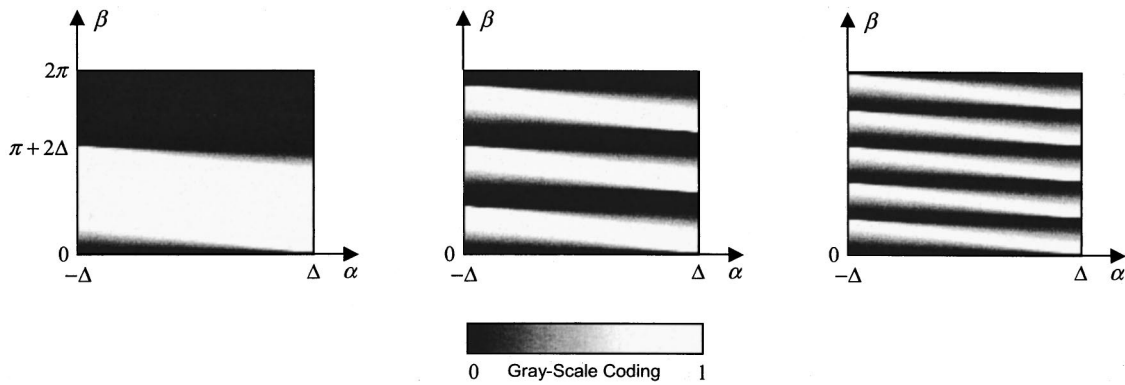


FIG. 5. Half-scan weighting functions in cases of multiple x-ray sources: (a) single x-ray source, (b) three x-ray sources, (c) five x-ray sources.

The half-scan Feldkamp-type cone-beam reconstruction was reported before in the case of a single x-ray source.^{7,8} By inserting the half-scan fan-beam weighting formula for an odd number of x-ray sources into a generalized Feldkamp reconstruction formula,⁶ we obtain the following cone-beam formula:

$$\begin{aligned}
 g(x, y, z) = & \frac{1}{2} \sum_{i=0}^{N-1} \int_{i(2\pi/N)}^{(i+1)(2\pi/N)} \frac{\rho^2(\beta)}{(\rho(\beta) - v)^2} \\
 & \times \int_{-\infty}^{\infty} w_i(p, \beta) R_i(\beta, p, \zeta) f\left(\frac{\rho(\beta)u}{\rho(\beta) - v} - p\right) \\
 & \times \frac{\rho(\beta)}{\sqrt{\rho^2(\beta) + p^2 + \zeta^2}} dp d\beta, \quad (3)
 \end{aligned}$$

where $g(x, y, z)$ denotes a reconstructed image, N is an odd number of x-ray sources, $\rho(\beta)$ the source-to-origin distance, $w_i(p, \beta)$ weighting functions, $R_i(\beta, p, \zeta)$ corresponding projection data, $i=0, 1, \dots, N-1$, and $f(\cdot)$ a reconstruction filter. Note that the weighting functions in the above-mentioned cone-beam formula assume equispacial data. These formulas can be directly obtained from those that assume equiangular data. Also, it is emphasized that the weighting functions remain the same in the cone-beam geometry, because Feldkamp-type reconstruction is essentially fan-beam reconstruction after cone-beam data are approximately corrected to fan-beam data.⁹ Because of the flexibility with the selection of the initial source angular position, the above-mentioned multi-source half-scan cone-beam formula can reconstruct an image volume at any time instant, as long as the source angular range meets the minimum requirement.

IV. NUMERICAL SIMULATION

The 3D Shepp and Logan’s phantom was used in the simulation. The phantom parameters are listed in Table I, where (x_0, y_0, z_0) specify the center of an ellipsoid, (a, b, c) denote the x, y, z semiaxes respectively, θ is the rotation angle around the z axis, and μ a relative linear x-ray attenuation coefficient. The effective x-ray attenuation coefficient at a point is the sum of the relative coefficients of the ellipsoids containing that point. In our numerical simulation, the multi-source fan-beam and cone-beam image reconstruction

software was developed in programming language Visual C++ (Microsoft Corporation) on a personal computer (800 MHz, 37.2 Gbytes, Dell Computer Corporation, Round Rock, TX).

First, we performed the multi-source half-scan fan-beam simulation, The length of the detector array was 512 cells. The number of projections was 400. The fan-beam angle was about 15°. The two-dimensional phantom was extracted at $z = -0.25$ from the 3D phantom as defined in Table I. Images were reconstructed on 512 by 512 matrices. Figure 6 shows (a) a full-scan reconstruction with one x-ray source, (b) a half-scan reconstruction with three x-ray sources, and (c) a half-scan reconstruction with five x-ray sources. It can be observed that the reconstructed results using multi-source half-scan fan-beam weighting functions have no significant difference in image quality as compared to the single-source full-scan counterpart. Note that the real gray level was transformed according to a linear relationship for better visualization. This transformation linearly maps the interval [0.95, 1.1] into 256 discrete gray levels. Truncation was done when necessary. The average of relative absolute errors was used to evaluate the multi-source half-scan fan-beam formula against the established full-scan fan-beam formula. The average of relative absolute errors is only about 0.1% in the fan-beam case, which indicates that the images produced using the new formula are in excellent agreement with that using the full-scan fan-beam formula.

Then, we performed the multi-source half-scan cone-beam simulation in a similar fashion. The detector plane was

TABLE I. Parameters of the 3D Shepp and Logan phantom.

No.	x_0	y_0	z_0	a	b	c	θ	τ
1	0.00	0.000	0.000	0.6900	0.920	0.900	0	2.00
2	0.00	0.000	0.000	0.6624	0.874	0.880	0	-0.98
3	-0.22	0.000	-0.250	0.4100	0.160	0.210	108	-0.02
4	0.22	0.000	-0.250	0.3100	0.110	0.220	72	-0.02
5	0.00	0.350	-0.250	0.2100	0.250	0.500	0	0.02
6	0.00	0.100	-0.250	0.0460	0.046	0.046	0	0.02
7	-0.08	-0.650	-0.250	0.0460	0.023	0.020	0	0.01
8	0.06	-0.650	-0.250	0.0460	0.023	0.020	90	0.01
9	0.06	-0.105	0.625	0.0560	0.040	0.100	90	0.02
10	0.00	0.100	0.625	0.0560	0.056	0.100	0	-0.02

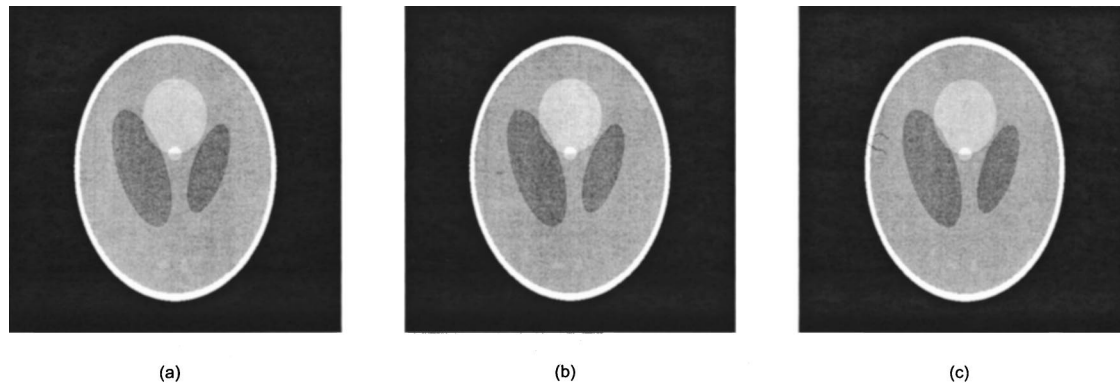


FIG. 6. Numerical simulation of half-scan fan-beam reconstruction. (a) Full-scan fan-beam reconstruction of the Shepp-Logan phantom at $z = -0.25$, (b) half-scan fan-beam reconstruction in the case of three x-ray sources, (c) half-scan fan-beam reconstruction in the case of five x-ray sources.

set to 2.2 by 2.2 with 256 by 256 detectors, its center was at the origin of the reconstruction coordinate system and its longitudinal axis was the z axis of the reconstruction coordinate system $x-y-z$. The number of projections was 200. Images were reconstructed on 256 by 256 matrices. In the simulation, a circular scanning locus was used, instead of a helical locus. Figure 7 shows (a) a Feldkamp reconstruction at $z = -0.25$ of the Shepp-Logan phantom, (b) a Feldkamp reconstruction of the same slice except that the largest bright ellipsoid was in a uniform horizontal motion, and (c) the corresponding five-source half-scan Feldkamp-type reconstruction. There was an evident motion blurring effect in Fig. 7(b), as indicated by the arrow. The blurring artifacts were basically eliminated using the five-source half-scan Feldkamp-type reconstruction, as demonstrated by the well-defined boundary of the largest bright ellipsoid in Fig. 7(c).

V. DISCUSSIONS AND CONCLUSION

After the multi-source half-scan weighting of projection data, the conventional filtered backprojection hardware and software can be directly used, because the principles for the design of the multi-source half-scan weighting scheme is the same as Parker's methodology. Specifically, the following regularity properties are required of the multi-source half-

scan weighting scheme: (1) the weighting function combines doubly sampled data into a unit contribution, (2) the weighting function is smooth in redundant regions, (3) both the weighting function and its first-order derivative are continuous at the boundaries of the redundant regions.

The speed improvement for such a multi-source system is significant. Quantitatively, the scanning angle would be $\pi/N + 2\Delta$, where Δ is the maximum fan-beam angle. In the case of $\Delta = 15^\circ$, the conventional single source would require a scan of 210° . On the other hand, it would take 90° for $N = 3$, and only 66° for $N = 5$. In other words, the speedup factor is 2.33 and 3.18 for three and five sources, respectively. Theoretically, a higher temporal resolution is always preferred. Practically, we consider that the number of sources can be three or five. A detailed justification is, however, beyond the scope of this paper.

The form of the half-scan weighting function is not unique. For single-source fan-beam CT, Crawford and King¹⁰ proposed a weighting function with a form different from that proposed by Parker.³ Such a weighting function can be generalized to multi-source fan-beam CT and multi-source cone-beam CT. Other forms of half-scan weighting functions may be explored in future studies, and optimized given a set of image quality requirements.

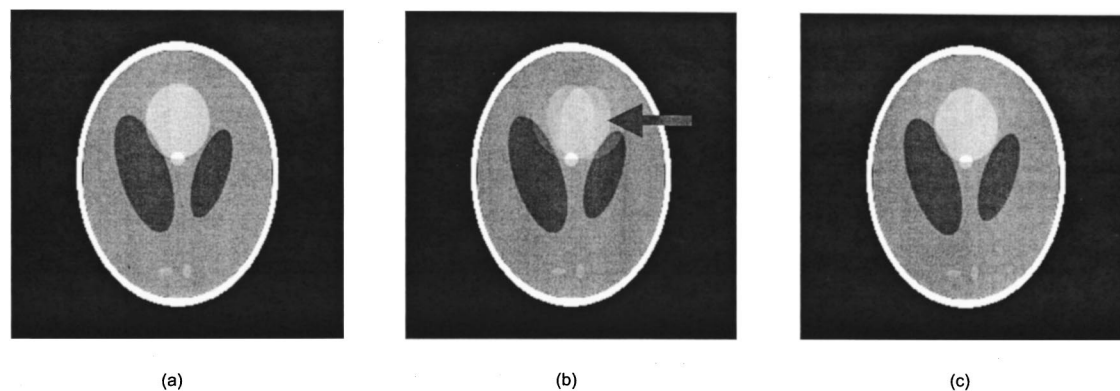


FIG. 7. Numerical simulation of half-scan cone-beam reconstruction. (a) Full-scan Feldkamp reconstruction of the 3D Shepp-Logan phantom at $z = -0.25$, (b) Feldkamp reconstruction of the phantom with a moving component (indicated by the arrow), (c) five-source half-scan cone-beam reconstruction corresponding to (b).

There are several practical issues with our proposed system. Artifacts may occur due to channel imbalance and geometric mismatches. The compensation means should be similar to what has been used for single-source scanners. As far as scattering is concerned, it would not be a major issue because the sample size is relatively small in our intended micro-CT application. A detailed study will be performed later to solve these problems and optimize the tradeoffs.

In conclusion, we have extended Parker's single-source half-scan weighting scheme to a multi-source half-scan version, and applied the generalized weighting scheme for half-scan Feldkamp-type reconstruction in the case of an odd number of x-ray sources. Due to the simultaneous data acquisition with multiple x-ray sources, the Feldkamp-type algorithm greatly improved temporal resolution without major artifacts in our numerical simulation. Such a system architecture may be valuable for dynamic/functional studies of both patients and small animals. Further work is needed to develop such a prototype system, apply the extended half-scan weighting scheme in other cone-beam algorithms,¹¹ and demonstrate the advantages of the improved temporal resolution in small animal studies and other applications.

ACKNOWLEDGMENT

This work was supported in part by grants from the National Institutes of Health (R43RR15325-01). A provisional patent application on this work was filed.

⁰Electronic mail: yliu@inav.net

¹M. J. Paulus, H. Sari-Sarraf, S. S. Gleason, M. Bobrek, J. S. Hicks, D. K. Johnson, J. K. Behel, L. H. Thompson, and W. C. Allen, "A new x-ray computed tomography system for laboratory mouse imaging," *IEEE Trans. Nucl. Sci.* **46**, 558–564 (1999).

²E. L. Ritman, R. A. Robb, and L. D. Harris, *Imaging Physiological Functions: Experience with the Dynamic Spatial Reconstructor* (Praeger, New York, 1985).

³D. L. Parker, "Optimal short scan convolution reconstruction for fan beam CT," *Med. Phys.* **9**, 254–257 (1982).

⁴L. A. Feldkamp, L. C. Davis, and J. W. Kress, "Practical cone-beam algorithm," *J. Opt. Soc. Am. A* **1**, 612–619 (1984).

⁵G. Wang, T. H. Lin, P. C. Cheng, D. M. Shinozaki, and H. Kim, "Scanning cone-beam reconstruction algorithms for x-ray microtomography," *Proc. SPIE* **1556**, 99–113 (1991).

⁶G. Wang, T. H. Lin, P. C. Cheng, and D. M. Shinozaki, "A general cone-beam reconstruction algorithm," *IEEE Trans. Med. Imaging* **12**, 486–496 (1993).

⁷G. T. Gullberg and G. L. Zeng, "A cone-beam filtered backprojection reconstruction algorithm for cardiac single photon emission computed tomography," *IEEE Trans. Med. Imaging* **11**, 91–101 (1992).

⁸G. Wang, Y. Liu, T. H. Lin, and P. C. Cheng, "Half-scan cone-beam x-ray microtomography formula," *J. Scanning Microscopy* **16**, 216–220 (1994).

⁹G. Wang, S. Y. Zhao, and P. C. Cheng, *Exact and Approximate Cone-beam X-ray Microtomography*, in *Modern Microscopies*, Vol. 1, edited by P. C. Cheng *et al.* (Springer, New York, 1999), pp. 233–261.

¹⁰C. R. Crawford and K. F. King, "Computed tomography scanning with simultaneous patient translation," *Med. Phys.* **17**, 967–982 (1990).

¹¹G. Wang, C. R. Crawford, and W. A. Kalender, "Multi-row-detector and cone-beam spiral/helical CT," *IEEE Trans. Med. Imaging* **19**, 817–821 (2000).